

FSUJ TPI QO-8/97

August, 1997

# Homodyne measurement of exponential phase moments

M. Dakna, T. Opatrný\*, D-G. Welsch

Friedrich-Schiller-Universität Jena Theoretisch-Physikalisches Institut

Max-Wien Platz 1, D-07743 Jena, Germany

## Abstract

It is shown that the exponential moments of the canonical phase can be directly sampled from the data recorded in balanced homodyne detection. Analytical expressions for the sampling functions are derived, which are valid for arbitrary states and bridge the gap between quantum and classical phase. The reconstruction of the canonical phase distribution from the experimentally determined exponential moments is discussed.

# 1 Introduction

Since Dirac's attempt in 1927 to introduce amplitude and phase operators in quantum mechanics [1] a number of concepts have been developed with the aim to overcome the problems resulting from the non-existence of a Hermitian phase operator (for a review, see [2]). Recently an attempt has been made to bridge the gap between two concepts which are based on essentially different approaches to the phase problem and widely used in quantum optics [3]. In the first, the phase of a radiation-field mode is defined from the requirement that phase and photon number should be complementary quantities. This first-principle definition leads to the *canonical phase* (also called London phase), the associated phase states being the right-hand eigenstates of a one-sided unitary exponential phase operator [4]. In the second, phase quantities are defined from the output observed in phase-sensitive measurements, such as eight-port homodyne detection. It is well known that in such a scheme the  $Q$  function [or, in the case of non-perfect detection, a smoothed  $Q$  function, i.e., an  $s$ -parametrized phase-space function with  $s < -1$ ] is measured [5, 6]. The *measured phase* distribution can then be obtained from radially integrating the (smoothed)  $Q$  function. Whereas in the classical limit the measured phase coincides with the canonical phase, in the quantum regime the two phases significantly differ from each other in general, because of the additional noise unavoidably connected with the  $Q$  function. So, from a study of the asymptotic behaviour of the measured and canonical phase distributions in the semiclassical domain it can be anticipated that the measured distribution is at least broader than the canonical one [3]. In the quantum regime it is principally not possible to obtain the canonical phase distribution from the radially integrated  $Q$  function, but it must be related to the complete quantum state, i.e., the complete  $Q$  function as a representation of the state in the phase space.

The best and perhaps ultimate method for measuring the quantum state of a traveling optical field has been four-port homodyne detection in which the quantum state is measured in terms of the quadrature-component distribution [7]. Since the quadrature-component distribution contains all knowable information on the quantum state, the various quantum-statistical properties of the system can be obtained from it. Moreover, the quadrature-component distribution is less noisy than the  $Q$  function and therefore it is more suitable for determining the quantum statistics than the  $Q$  function. The method also called *optical homodyne tomography* (OHT) was first used for reconstructing the Wigner function of a single-mode optical field applying inverse Radon transform [8], which requires a three-fold integration of the measured data. In the numerical calculation the standard filtered back projection algorithm is usually used, so that the reconstruction of the Wigner function is biased by data filtering.

This problem does not appear and the effort is drastically reduced if the quantities that one is interested in can be directly sampled from the homodyne

data. In particular, the determination of the quantities and the error estimation are very fast and can be performed in *real time*. Systematic errors can easily be reduced to any desired degree of accuracy and the remaining statistical errors only reflect the finite number of measurement events. It has been shown that both the density matrix in the photon-number basis [9] and the moments and correlations of the photon creation and destruction operators [10] can be obtained in this way, which has offered novel possibilities of the experimental determination of the photon-number statistics of light.

In contrast to the photon-number statistics, the determination of the canonical phase statistics has been an open problem. The phase statistics can of course be tried to be determined indirectly by calculating it approximately from the Wigner function, using in the reconstruction of the Wigner function the standard filtered back projection algorithm of inverse Radon transformation [11]. Another indirect method, which avoids the rather lengthy detour via the Wigner function, is the calculation of the phase statistics from the sampled density matrix in the photon-number basis [12]. However, since canonical phase and photon number are complementary quantities, there is no *a priori* upper bound for the density-matrix elements that can contribute to the phase statistics. Hence, large numbers of density-matrix elements must be sampled, the statistical errors of which then give rise to an error accumulation in the phase statistics such that the inaccuracies eventually dominate the result (note that the statistical error of the off-diagonal density-matrix elements increases with the distance from the diagonal). To limit the effect of inaccuracies, one must necessarily restrict the method to states of low photon numbers and appropriately truncate them. A way that remains to overcome the problem is to directly sample the phase statistics from the homodyne data. Unfortunately the canonical phase distribution cannot be related to the quadrature-component distribution in the sense of a sampling formula because the corresponding integral kernel does not exist. It has been therefore suggested to introduce the exact phase distribution as the limit of a convergent sequence of appropriately parametrized (smeared) distributions each of which can directly be sampled from the homodyne data [13]. The exact phase distribution can then be obtained asymptotically to any degree of accuracy, if the sequence parameter is chosen such that smearing is suitably weak. In practice it is therefore required that the sampling procedure is performed simultaneously for various values of the sequence parameter, each value giving rise to its own sampling function. The disadvantage of the method is rather technical, since the numerical effort drastically increases with the number of photons contained in a state. This fact makes the method effectively applies only to states with low photon numbers. Finally, it has been suggested to measure the canonical phase distribution asymptotically by replacing the local-oscillator in the homodyne detection scheme with a reference mode prepared in so-called reciprocal binomial states – a method that is also state dependent and hardly realizable at present [14].

In this paper we show that the problem of direct determination of the canonical phase statistics from the homodyne data can be solved when it is based on the exponential phase moments (i.e., the Fourier components of the phase distribution) and not on the phase distribution itself. We show that the exponential phase moments can be directly sampled from the quadrature-component distribution, without making a detour via other quantities and without any assumptions and approximations with regard to the state. In particular, we derive analytical expression for the sampling functions and give a very simple procedure for the numerical calculation. Since the method is independent of the state, it applies to both quantum and classical fields and all fields in between in a unified way and bridges, through the universally valid sampling functions, the gap between quantum and classical phase. Needless to say that for obtaining the full information on the phase statistics, all (non-vanishing) exponential phase moments must be determined. It is worth noting that already sampling of a few low-order moments provide us with interesting information [15].

The paper is organized as follows. In Sec. 2 the problem of direct sampling of the exponential phase moments of a classical oscillator from the quadrature-component distribution is studied. In Sec. 3 the theory is extended to the canonical phase of a quantum oscillator. Measurement errors are studied in Sec. 4, and in Sec. 5 numerical results of computer simulations of measurements for determining the canonical phase statistics are presented. Lengthy mathematical derivations are given in appendices.

## 2 Sampling of exponential phase moments – classical case

In order to gain insight into the problem of phase measurement by means of balanced homodyne detection, let us first consider the situation in classical optics. Here we can assume a proper phase-space probability  $W(q, p) dqdp$ , which can be rewritten as, on introducing polar coordinates  $q = r \cos \varphi$  and  $p = r \sin \varphi$ ,

$$W(q, p) dqdp = P(r, \varphi) drd\varphi, \quad (1)$$

where

$$P(r, \varphi) = r W(r \cos \varphi, r \sin \varphi). \quad (2)$$

The phase probability distribution  $P(\varphi)$  is then defined by

$$P(\varphi) = \int_0^\infty dr P(r, \varphi), \quad (3)$$

and the exponential phase moments  $\Psi_k$ , which are given by the Fourier components of the phase probability distribution,

$$\Psi_k = \int_{2\pi} d\varphi e^{ik\varphi} P(\varphi), \quad (4)$$

can be written as

$$\Psi_k = \int_{2\pi} d\varphi \int_0^\infty dr e^{ik\varphi} P(r, \varphi). \quad (5)$$

In balanced homodyne detection the probability distributions  $p(x, \vartheta)$  for the field quadratures  $x(\vartheta) = q \cos \vartheta + p \sin \vartheta$  are measured. [Note that when the harmonic oscillator represents a moving particle in a harmonic potential, then  $\vartheta = \omega t$  is valid and  $x(\omega t)$  is the time-dependent position of the particle.] The quadrature-component probability distribution  $p(x, \vartheta)$  can be obtained from the phase-space probability distribution  $P(r, \varphi)$  as, on recalling that  $x(\vartheta) = r \cos(\varphi - \vartheta)$ ,

$$p(x, \vartheta) = \int_{2\pi} d\varphi \int_0^\infty dr P(r, \varphi) \delta[x - r \cos(\varphi - \vartheta)], \quad (6)$$

which is nothing but the well-known Radon transform, whose inversion yields the phase-space probability distribution in terms of the quadrature-component distribution.

Let us now turn to the problem of direct sampling of the exponential phase moments. A quantity  $\mathcal{A}$  can be determined from the homodyne data by means of the sampling method, if it can be related to  $p(x, \vartheta)$  as

$$\mathcal{A} = \int_{2\pi} d\vartheta \int_{-\infty}^\infty dx K_{\mathcal{A}}(x, \vartheta) p(x, \vartheta) \quad (7)$$

with a well-behaved integral kernel  $K_{\mathcal{A}}(x, \vartheta)$  as sampling function. Note that  $p(x, \vartheta + \pi) = p(-x, \vartheta)$ , so that the  $\vartheta$  integration in Eq. (8) can be restricted to a  $\pi$  interval. For the sake of convenience, here and in the following we prefer a  $2\pi$  interval. In contrast to the full phase-space probability distribution  $P(r, \varphi)$ , which cannot be obtained from  $p(x, \vartheta)$  by a simple inversion of Eq. (6) in the form of Eq. (7), the sampling method applies to the Fourier components of the radially integrated phase-space probability distribution, i.e., the exponential phase moments  $\Psi_k$  can be given by

$$\Psi_k = \int_{2\pi} d\vartheta \int_{-\infty}^\infty dx K_k(x, \vartheta) p(x, \vartheta). \quad (8)$$

Substituting in Eq. (8) for  $p(x, \vartheta)$  the expression (6), we arrive at

$$\Psi_k = \int_{2\pi} d\vartheta \int_{2\pi} d\varphi \int_{-\infty}^\infty dx \int_0^\infty dr K_k(x, \vartheta) P(r, \varphi) \delta[x - r \cos(\varphi - \vartheta)]. \quad (9)$$

In order to determine the integral kernel  $K_k(x, \vartheta)$ , it is convenient to introduce the Fourier decomposition

$$K_k(x, \vartheta) = \sum_{l=-\infty}^{\infty} e^{il\vartheta} K_{k,l}(x). \quad (10)$$

When the phase argument  $\varphi$  in  $P(r, \varphi)$  is shifted towards  $\varphi + \varphi_0$ , i.e.,  $P(r, \varphi) \rightarrow P(r, \varphi + \varphi_0)$ , then it follows from Eq. (5) that  $\Psi_k$  changes as  $\Psi_k \rightarrow e^{-ik\varphi_0}\Psi_k$ . Comparing this requirement with Eqs. (9) and (10), we find that  $K_{k,l}(x)$  must be of the form  $K_{k,l}(x) = \delta_{k,l}K_k(x)$ , and hence

$$K_k(x, \vartheta) = e^{ik\vartheta}K_k(x). \quad (11)$$

We now insert this expression into Eq. (9), compare the result with Eq. (5) and find that  $K_k(x)$  must satisfy the integral equation

$$\int_{2\pi} d\varphi e^{ik\varphi} K_k(r \cos \varphi) = 1 \quad (12)$$

for all  $r > 0$ .

From Eq. (12) we can see that  $K_k(x)$  is not uniquely defined. First, any function of parity  $(-1)^{k+1}$  can be added to  $K_k(x)$  without changing the integral. Second, any polynomial of a degree less than  $k$  can also be added to  $K_k(x)$ . As can be verified by direct substitution, a solution of Eq. (12) for odd and even  $k$ , respectively, is given by

$$K_{2m+1}(x) = \frac{1}{4}(-1)^m(2m+1)\text{sign}(x) \quad (13)$$

and

$$K_{2m}(x) = \pi^{-1}(-1)^{m+1}m \ln |x| + C \quad (14)$$

[ $m = 0, 1, 2, \dots$ , where  $C$  is an (irrelevant) constant.] Note that this solution ensures that the integral (8) exists for any quadrature-component distribution  $p(x, \vartheta)$  which with increasing  $|x|$  decreases at least as  $|x|^{-(1+\epsilon)}$ ,  $\epsilon$  being a (arbitrarily small) positive constant, i.e., for any physical state. Clearly, this would be not the case if, within the ambiguity mentioned, polynomials were added to the functions (13) and (14). Another reason for choosing the functions (13) and (14) is the reduction of the statistical error in a real experiment. Since this error is related to the variance of the kernel (Sec. 4.3), it is advantageous to choose kernels which are varying as slowly as possible.

### 3 Sampling of exponential phase moments – quantum case

It is worth noting that the results derived in Sec. 2 also remain valid for a quantized radiation-field mode, provided that  $W(q, p)$  [or in polar coordinates,  $P(r, \varphi)$ ] is identified with the quantum-mechanical Wigner function. Hence, using in Eqs. (9) and (11) the functions (13) and (14) enables one to determine exponential phase moments defined by the Fourier components of the radially integrated

Wigner function from the homodyne data by means of the sampling method. Since the Wigner function of a quantum oscillator can attain negative values, it cannot be regarded, in general, as a proper phase-space probability distribution, and hence the radially integrated Wigner function does not represent, in general, a proper phase distribution function.

As already mentioned, for a quantized radiation-field mode photon number and canonical phase are complementary variables, and in place of Eq. (3) we have

$$P(\varphi) = (2\pi)^{-1} \langle \varphi | \hat{\varrho} | \varphi \rangle, \quad (15)$$

where  $\hat{\varrho}$  and  $|\varphi\rangle$ , respectively, are the density operator of the state and the (un-normalizable) phase states [16]

$$|\varphi\rangle = \sum_{n=0}^{\infty} e^{in\varphi} |n\rangle, \quad (16)$$

which are right-hand eigenstates of the only one-sided unitary operator

$$\hat{E} = (\hat{n} + 1)^{1/2} \hat{a}, \quad (17)$$

$$\hat{E} |\varphi\rangle = e^{i\varphi} |\varphi\rangle. \quad (18)$$

In Eq. (17),  $\hat{n} = \hat{a}^\dagger \hat{a}$  is the photon-number operator,  $\hat{a}^\dagger$  and  $\hat{a}$  being the photon creation and annihilation operators, respectively. From Eqs. (15) and (18) together with the fact that the phase states resolve the unity it is easily seen that the exponential phase moments  $\Psi_k$  defined in Eq. (4) can be written as

$$\Psi_k = \langle \hat{E}^k \rangle \quad (19)$$

for  $k = 1, 2, \dots$ , and  $\Psi_k = \Psi_{-k}^*$  for  $k = -1, -2, \dots$ . We now combine Eqs. (17) and (19) and obtain [in place of Eq. (5)]

$$\Psi_k = \sum_{n=0}^{\infty} \varrho_{n+k,n} \quad (20)$$

( $k = 1, 2, \dots$ ). Next, we express the quadrature-component distribution

$$p(x, \vartheta) = \langle x, \vartheta | \hat{\varrho} | x, \vartheta \rangle \quad (21)$$

in terms of the density-matrix elements in the photon-number basis. For this purpose we expand in Eq. (21) the eigenstates  $|x, \vartheta\rangle$  of the quadrature-component operator  $\hat{x}(\vartheta) = 2^{-1/2} (e^{-i\vartheta} \hat{a} + e^{i\vartheta} \hat{a}^\dagger)$  in the photon-number basis [17],

$$|x, \vartheta\rangle = \sum_{n=0}^{\infty} e^{in\vartheta} \psi_n(x) |n\rangle, \quad (22)$$

where the functions  $\psi_n(x)$  are the eigenfunctions of the harmonic-oscillator Hamiltonian,  $\psi_n(x) = (2^n n! \sqrt{\pi})^{-1/2} \exp(-x^2/2) H_n(x)$ ,  $H_n(x)$  being the Hermite polynomial. From Eqs. (21) and (22) we then obtain [in place of Eq. (6)]

$$p(x, \vartheta) = \sum_{n=0}^{\infty} \sum_{m=0}^{\infty} \psi_n(x) \psi_m(x) \varrho_{m,n} e^{i(n-m)\vartheta}. \quad (23)$$

Let us again assume that  $\Psi_k$  can be obtained from  $p(x, \vartheta)$  according to Eq. (8). Substituting in Eq. (8) for  $p(x, \vartheta)$  the quantum-mechanical expression (23) and comparing the result with Eq. (20), we see that the kernel  $K_k(x, \vartheta)$  must be of the form (11), but now  $K_k(x)$  must satisfy the integral equation

$$2\pi \int_{-\infty}^{\infty} dx K_k(x) \psi_{n+k}(x) \psi_n(x) = 1 \quad (24)$$

( $n = 0, 1, 2, \dots$ ). Equation (24) plays the same role for a quantum oscillator as Eq. (12) for a classical oscillator does. From Eq. (24) and the properties of the Hermite polynomials the same ambiguity in the determination of  $K_k(x)$  as in the classical case (Sec. 2) is found. Provided that a  $K_k(x)$  exists, any function of parity  $(-1)^{k+1}$  and/or any polynomial of a degree less than  $k$  can be added to  $K_k(x)$  in order to again obtain a solution of Eq. (24).

We now turn to the problem of construction of an integral kernel that satisfies Eq. (24). For this purpose we return to Eq. (19) and bring the operator  $\hat{E}^k$  into the normally ordered form,

$$\begin{aligned} \hat{E}^k &= \sum_{n=0}^{\infty} : \frac{\hat{a}^{\dagger n} \exp(-\hat{a}^{\dagger} \hat{a}) \hat{a}^{n+k}}{\sqrt{n!(n+k)!}} : \\ &= \sum_{n=0}^{\infty} \sum_{m=0}^{\infty} \frac{1}{\sqrt{n!(n+k)!}} \frac{(-1)^m}{m!} \hat{a}^{\dagger n+m} \hat{a}^{n+m+k} \end{aligned} \quad (25)$$

(the notation  $: :$  is used to indicate normal ordering). From the expansion (25) together with the sampling formula for normally ordered moments and correlations of the photon creation and annihilation operators [10],

$$\langle \hat{a}^{\dagger n} \hat{a}^m \rangle = \left[ 2\pi \sqrt{2^{n+m}} \binom{n+m}{m} \right]^{-1} \int_{2\pi} d\vartheta \int_{-\infty}^{\infty} dx e^{i(n-m)\vartheta} H_{n+m}(x) p(x, \vartheta), \quad (26)$$

we find after some calculation (see Appendix A) that  $\Psi_k$ , Eq. (19), can be written in the form of Eq. (8),

$$\Psi_k = \int_{2\pi} d\vartheta \int_{-\infty}^{\infty} dx \tilde{K}_k(x) e^{ik\vartheta} p(x, \vartheta). \quad (27)$$

In Eq. (27), the integral kernel  $\tilde{K}_k(x)$  can be decomposed into two parts,

$$\tilde{K}_k(x) = K_k(x) - F_k(x), \quad (28)$$



where for odd and even  $k$ , respectively,  $K_k(x)$  reads as

$$K_{2m+1}(x) = (-1)^m \frac{2x(m+1)!}{(2\pi)^{m+3/2}} \int_0^{+\infty} dr \left\{ \Omega^{(2m+1)}(r^2) \times \frac{r^{2m} \Phi[m+2, 3/2, -x^2 \tanh(r^2/2)]}{e^{-(m+1)r^2} \sinh^m(r^2/2) \cosh^{m+2}(r^2/2)} \right\} \quad (29)$$

and

$$K_{2m}(x) = (-1)^m \frac{m!}{(2\pi)^{m+1}} \int_0^{+\infty} dr \left\{ \Omega^{(2m)}(r^2) \times \frac{r^{2m-1} e^{mr^2/2}}{\sinh^m(r^2/2)} \left[ \frac{\Phi[m+1, 1/2, -x^2 \tanh(r^2/2)]}{e^{-(m+1)r^2/2} \cosh^{m+1}(r^2/2)} - 1 \right] \right\}, \quad (30)$$

and  $F_k(x)$  is the polynomial

$$F_k(x) = \frac{1}{2\pi 2^{k/2}} \sum_{n=1}^{\lfloor \frac{k-1}{2} \rfloor} \left[ \frac{(-2)^n (k-n)!}{(k-2n)!} H_{k-2n}(x) \times \sum_{l=0}^{\infty} \binom{n+l-1}{l} \frac{1}{\sqrt{(l+1) \dots (l+k)}} \right]. \quad (31)$$

In Eqs. (29) and (30),  $\Phi(a, b, y)$  is the confluent hypergeometric function and  $\Omega^{(k)}(z)$  defined in Eq. (A 18) [together with Eq. (A 17)] in Appendix A can be given by power-series expansion (Appendix B),

$$\Omega^{(k)}(z) = \sum_{m=0}^{\infty} A_m^{(k)} z^m, \quad (32)$$

where

$$A_m^{(k)} = \frac{(-1)^m}{m!} \frac{2\pi^{k/2}}{\Gamma(k/2 + m)} \frac{\partial^m}{\partial x^m} \left[ \prod_{j=1}^k (1 - jx)^{-\frac{1}{2}} \right] \Big|_{x=0}. \quad (33)$$

From Eqs. (29) – (31) [together with Eq. (A 18)] it is seen that  $\tilde{K}_k(x)$  exists, and it can be proved by direct substitution that  $\tilde{K}_k(x)$  satisfies Eq. (24). Hence we have found a solution of Eq. (24) even when the assumption made for constructing it fails (i.e., when the moments and correlations (26) do not exist for all  $m$  and  $n$ , see the derivation in Appendix A). It is worth noting that both  $\tilde{K}_k(x)$  and  $K_k(x)$  are solutions of Eq. (24), because the polynomial  $F_k(x)$  in Eq. (28) reflects the above mentioned ambiguity in the solution of Eq. (24) and can therefore be omitted. Further, it can be shown (Appendix C) that with increasing  $|x|$  the solution  $K_k(x)$  approaches the classical one, i.e., the asymptotic behavior for large  $|x|$  of Eqs. (29) and (30), respectively, is exactly given by Eq. (13) and

Eq. (14). We see that  $K_k(x)$  can be used for determining exponential phase moments from the homodyne data for all states whose quadrature-component distributions  $p(x, \vartheta)$  asymptotically decrease at least as  $|x|^{-(1+\epsilon)}$ ,  $\epsilon > 0$ , i.e., for any physical state. Since  $K_k(x)$  applies to both quantum and classical systems in a unified way, the sampling method bridges the gap between quantum and classical phase. Examples of  $K_k(x)$  for various  $k$  are shown in Fig. 1. It is seen that they are well-behaved functions, which rapidly approach the classical limit and differ from it only in the small region of vacuum fluctuations.

Let us comment on the numerical calculation of  $K_k(x)$  which can be performed in a straightforward manner. In particular, from Eqs. (29) and (30), respectively, it can be easily proved that [15, 18]

$$K_1(x) = \pi^{-3/2} x \int_0^\infty \frac{dt}{\sqrt{t} \cosh^2 t} \Phi\left(2, \frac{3}{2}, -x^2 \tanh t\right) \quad (34)$$

and [after calculating  $\Omega^{(2)}(r^2)$  according to Eq. (A 18)] [15]

$$K_2(x) = \frac{1}{2\pi} \int_0^\infty dt I_0(t) \left[ \frac{e^{-2t}}{\sinh t} - \frac{1}{\cosh^2 t \sinh t} \Phi\left(2, \frac{1}{2}, -x^2 \tanh t\right) \right] \quad (35)$$

[ $I_0(t)$ , modified Bessel function]. The one-dimensional integrals can then be calculated numerically using standard methods. In order to calculate  $K_k(x)$  for arbitrary  $k$  it may be convenient to start from  $\tilde{K}_k(x)$  as given in Eq. (A 2) in Appendix A and approximate it in a small (nonclassical) interval by a finite sum such that

$$K_k(x) \approx (2\pi)^{-1} \sum_{l=0}^{l_0} C_l^{(k)} H_{2l+k}(x) + F_k(x), \quad |x| < x_0, \quad (36)$$

and use the classical limit, Eqs. (13) and (14), elsewhere. For example, for the calculation of the kernels plotted in Fig. 1 it is sufficient to choose the parameters  $l_0 = 40$  and  $x_0 = 4$ , and to truncate the infinite sum in Eq. (31) for  $F_k(x)$  at  $l = 10^3$ .

## 4 Nonperfect detection and measurement errors

In practice there is always a number of experimental inaccuracies that limit the precision with which the exponential phase moments can be determined. In this section we restrict attention to three kinds of inaccuracies: data smearing, discretization of the phase parameter  $\vartheta$ , and finite number of measurement events (i.e., discretization of  $x$ ).

## 4.1 Data smearing

Since in a realistic experiment the quadrature components cannot be measured with infinite precision, we may assume that instead of  $p(x, \vartheta)$  a smeared distribution

$$p(x, \vartheta; \eta) = \int_{-\infty}^{\infty} dy f(x - y; \eta) p(y, \vartheta) \quad (37)$$

is obtained. In Eq. (37),  $f(x; \eta)$  is some positive single-peaked function and  $\eta$  is a parameter quantifying the smearing effect. A typical example of  $f(x; \eta)$  is a Gaussian, such as

$$f(x; \eta) = \frac{1}{\sqrt{2\pi\sigma^2}} \exp\left(-\frac{x^2}{2\sigma^2}\right), \quad \sigma^2 = \frac{1 - \eta}{2\eta}, \quad (38)$$

which corresponds to the use of nonperfect photodetectors whose efficiency  $\eta$  is less than unity.

Substituting in Eq. (8) for the exact distribution  $p(x, \vartheta)$  the smeared distribution  $p(x, \vartheta; \eta)$  yields exponential phase moments  $\Psi_k(\eta)$  that differ from  $\Psi_k$  in a systematic error (bias)  $\Delta^{(s)}\Psi_k$  as follows:

$$\Psi_k(\eta) = \int_{2\pi} d\vartheta \int_{-\infty}^{\infty} dx K_k(x, \vartheta) p(x, \vartheta; \eta) = \Psi_k + \Delta^{(s)}\Psi_k \quad (39)$$

with

$$\Delta^{(s)}\Psi_k = \int_{2\pi} d\vartheta e^{ik\vartheta} \int_{-\infty}^{\infty} dx g_k(x; \eta) p(x, \vartheta), \quad (40)$$

where

$$g_k(x; \eta) = \int_{-\infty}^{\infty} dy K_k(y) [f(y - x; \eta) - \delta(y - x)]. \quad (41)$$

Examples of the kernel  $g_k(x; \eta)$  for the determination of the systematic error  $\Delta^{(s)}\Psi_k$  are plotted in Fig. 2 [with  $f(x; \eta)$  according to Eq. (38)]. From a comparison of  $g_k(x; \eta)$  with  $K_k(x)$  (see Figs. 1 and 2) it is expected that the absolute values of  $\Psi_k(\eta)$  are smaller than those of  $\Psi_k$  in general. The systematic error is state-dependent as it can be seen from Eq. (40). To give an impression of its magnitude, let us restrict attention to the classical limit and consider a state whose phase-space probability distribution is radially sharply localized at  $r = r_0$  such that  $r_0 \gg \sigma$ . In this case it can be shown that, on assuming Gaussian smearing and using the results in Sec. 2,

$$\Psi_k(\eta) \approx \exp\left(-\frac{k^2\sigma^2}{2r_0^2}\right) \Psi_k, \quad (42)$$

which reveals that the exponential phase moments can be determined from the smeared data quite reliably as long as  $k \ll r_0/\sigma$ .

It is worth noting that under certain circumstances it is possible to compensate for the systematic error during the sampling process, introducing an appropriately modified kernel  $K_k(x; \eta)$ . Let us again assume Gaussian smearing, which is typically observed in nonperfect detection, and apply Eq. (37) together with Eq. (38). In this case we may replace Eq. (26) with [18]

$$\langle \hat{a}^{\dagger n} \hat{a}^m \rangle = \left[ 2\pi \sqrt{(2\eta)^{n+m}} \binom{n+m}{m} \right]^{-1} \times \int_{2\pi} d\vartheta \int_{-\infty}^{\infty} dx e^{i(n-m)\vartheta} H_{n+m}(x) p(x, \vartheta; \eta), \quad (43)$$

and follow the lines given in Sec. 3 and Appendix A. It is easily seen that in Eq. (27)  $p(x, \vartheta)$  and  $\tilde{K}_k(x)$ , respectively, must be replaced with  $p(x, \vartheta; \eta)$  and  $\tilde{K}_k(x; \eta)$ , provided that  $\tilde{K}_k(x; \eta)$  exists. The kernel  $\tilde{K}_k(x; \eta)$  obviously compensates for the losses associated with nonperfect detection and can be obtained from Eq. (A 2) in Appendix A, if  $C_l^{(k)}$  is replaced with  $C_l^{(k)}(\eta) = \eta^{-(l+k/2)} C_l^{(k)}$ . In close analogy to Eq. (28) we then find that the modified kernel  $\tilde{K}_k(x; \eta)$  can be rewritten as

$$\tilde{K}_k(x; \eta) = K_k(x; \eta) - F_k(x; \eta), \quad (44)$$

where for even and odd  $k$ , respectively,  $\eta^{k/2} K_k(x; \eta)$  is given by Eqs. (A 16) and (A 15), if in the integrals  $z_k$  is replaced with  $z_k(\eta) = z_k/\eta$ . Finally, Eqs. (29) and (30), respectively, are replaced with

$$K_{2m+1}(x; \eta) = (-1)^m \frac{2x(m+1)!}{(2\pi/\eta)^{m+3/2}} \int_0^{+\infty} dr \left\{ \Omega^{(2m+1)}(r^2) \times \frac{r^{2m} \Phi[m+2, 3/2, -x^2 \lambda(r^2; \eta) \tanh(r^2/2)]}{e^{-(m+1)r^2} \sinh^m(r^2/2) [\lambda(r^2; \eta) \cosh(r^2/2)]^{m+2}} \right\} \quad (45)$$

and

$$K_{2m}(x; \eta) = (-1)^m \frac{m!}{(2\pi/\eta)^{m+1}} \int_0^{+\infty} dr \left\{ \Omega^{(2m)}(r^2) \times \frac{r^{2m-1} e^{mr^2/2}}{\sinh^m(r^2/2)} \left[ \frac{\Phi[m+1, 1/2, -x^2 \lambda(r^2; \eta) \tanh(r^2/2)]}{e^{-(m+1)r^2/2} [\lambda(r^2; \eta) \cosh(r^2/2)]^{m+1}} - 1 \right] \right\}, \quad (46)$$

where

$$\lambda(r^2; \eta) = 1 + (\eta - 1)(1 + e^{-r^2})^{-1}, \quad (47)$$

and the polynomial  $F_k(x; \eta)$  reads as

$$F_k(x; \eta) = \frac{1}{2\pi(2\eta)^{k/2}} \sum_{n=1}^{\lfloor \frac{k-1}{2} \rfloor} \left[ \frac{(-2\eta)^n (k-n)!}{(k-2n)!} H_{k-2n}(x) \times \sum_{l=0}^{\infty} \binom{n+l-1}{l} \frac{1}{\sqrt{(l+1) \dots (l+k)}} \right]. \quad (48)$$

Needless to say that the polynomial can again be omitted since both  $\tilde{K}_k(x; \eta)$  and  $K_k(x; \eta)$  are solutions of the problem and in practical measurements  $K_k(x; \eta)$  is more suited for error reduction than  $\tilde{K}_k(x; \eta)$ . The numerical calculation of  $K_k(x; \eta)$  can be performed in a way as outlined in Sec. 3 for  $K_k(x)$ . Examples of  $K_k(x; \eta)$  for various values of  $k$  and  $\eta$  are shown in Fig. 3.

It should be pointed out that the sum rules (A 13) and (A 14) used in the derivation only apply when  $|z_k(\eta)| < 1$ . Hence we observe that the condition  $\eta > 1/2$  must be fulfilled in order to compensate for Gaussian data smearing, which is analogous to the density matrix reconstruction in the Fock basis [9]. It is worth noting that the condition  $\eta > 1/2$  corresponds to the requirement that the width of the Gaussian (38) is smaller than the vacuum noise. From Fig. 3 we see that with increasing  $|x|$  the kernel  $K_k(x; \eta)$  for odd  $k$  rapidly approaches the classical limit (13) for perfect detection, whereas for even  $k$  it approaches the classical limit (14) up to an irrelevant  $\eta$ -dependent constant. The results reveal that in classical optics it is impossible to compensate for the losses in nonperfect detection, because of the vanishing vacuum noise of a classical oscillator.

As expected, substantial differences between  $K_k(x; \eta)$  and  $K_k(x)$  are observed in the region around  $x=0$ , and they increase with decreasing  $\eta$  (Fig. 3). The [compared with  $K_k(x)$ ] stronger variation of  $K_k(x; \eta)$  implies that the use of  $K_k(x; \eta)$  for sampling of the exponential phase moments from the smeared quadrature-component distribution gives rise to a larger statistical error than the use of  $K_k(x)$  (for the statistical error, see Sec. 4.3). This is obviously the price paid for suppression of the systematic error. Based on the precision of the data available, the experimenter should therefore decide whether to use  $K_k(x; \eta)$  (which increases the statistical error) or  $K_k(x)$  (which decreases the statistical error but introduces a bias).

## 4.2 Phase discretization

In practice,  $p(x, \vartheta)$  can only be measured at  $N$  discrete phases  $\vartheta_l$ . When they are equidistantly distributed over a  $2\pi$  interval, i.e.,  $\vartheta_l = (2\pi/N)l$ , where  $l = 0, 1, \dots, N-1$ , then application of Eq. (8) yields the experimentally determined exponential phase moments

$$\Psi_k(N) = \frac{2\pi}{N} \sum_{l=0}^{N-1} e^{ik\vartheta_l} \int_{-\infty}^{\infty} dx K_k(x) p(x, \vartheta_l), \quad (49)$$

which can be rewritten as, on using Eq. (23),

$$\Psi_k(N) = \frac{2\pi}{N} \sum_{l=0}^{N-1} \sum_{m,n=0}^{\infty} e^{i\frac{2\pi}{N}(k+n-m)l} \varrho_{m,n} \int_{-\infty}^{\infty} dx K_k(x) \psi_m(x) \psi_n(x). \quad (50)$$

Taking into account that  $N^{-1} \sum_{l=0}^{N-1} e^{i2\pi(k+n-m)l/N} = \delta_{k+n-m \bmod N}$  and recalling Eqs. (20) and (24), we derive

$$\Psi_k(N) = \Psi_k + \Delta\Psi_k^{(d)}, \quad (51)$$

where

$$\Delta\Psi_k^{(d)} = \sum_{s=1}^{\infty} \sum_{n=0}^{\infty} \left( \varrho_{n+k+sN,n} Q_{n+k+sN,n}^{(k)} + \varrho_{n,n+sN-k} Q_{n,n+sN-k}^{(k)} \right) \quad (52)$$

represents the systematic error owing to phase discretization. In Eq. (52) the abbreviation

$$Q_{m,n}^{(k)} = 2\pi \int_{-\infty}^{\infty} dx K_k(x) \psi_m(x) \psi_n(x) \quad (53)$$

is used and it is assumed, for notational convenience, that  $N > k$ . Note that from physical arguments it is also reasonable to assume that the number of phases is larger than the index of the measured moment (otherwise the systematic error could dominate the result).

From Eq. (52) we see that the error is influenced by all off-diagonal density-matrix elements of the type of  $\varrho_{n+k\pm sN,n}$ . The effect, which is also called “aliasing”, has also been found in the reconstruction of the density matrix in the Fock basis from the data measured in balanced [19] and unbalanced [20] homodyning. For highly excited states (i.e.,  $\hat{\varrho}_{n,m} \approx 0$  if  $n, m < n_0$ , with  $n_0 \gg 1$ ) the relevant  $Q_{m,n}^{(k)}$  can be approximately calculated, using in Eq. (53) the classical kernel given in Eqs. (13) and (14):

$$Q_{n+k+sN,n}^{(k)} \approx (-1)^{Ns/2} \frac{k}{sN+k}, \quad Q_{n,n+sN-k}^{(k)} \approx -Q_{n-k+sN,n}^{(k)}, \quad (54)$$

Note that  $sN$  is even, since from the symmetry properties of  $Q_{m,n}^{(k)}$  it follows that  $Q_{m,n}^{(k)} = 0$  if  $m+n+k$  is odd. Combining Eqs. (52) and (54) yields

$$\Delta\Psi_k^{(d)} \approx \sum_{s=1}^{\infty} (-1)^s \left( \frac{k}{2sN+k} \Psi_{k+2Ns} + \frac{k}{2sN-k} \Psi_{k-2Ns} \right) \quad (55)$$

for odd  $N$  and

$$\Delta\Psi_k^{(d)} \approx \sum_{s=1}^{\infty} (-1)^{Ns/2} \left( \frac{k}{sN+k} \Psi_{k+Ns} + \frac{k}{sN-k} \Psi_{k-Ns} \right) \quad (56)$$

for even  $N$ . We see that the error of the measured exponential phase moment is expressed in terms of higher-order moments, and it decreases with increasing  $N$ . Note that the difference between the errors in Eqs. (55) and (56) reflects the fact that with regard to a  $\pi$  interval, the number of different phases is twice as large for odd  $N$  as for even  $N$ , which of course substantially reduces the systematic error in the first case.

### 4.3 Statistical error

When in an experiment  $n(\vartheta_l)$  measurements are performed for each phase  $\vartheta_l$ , the exponential phase moments can be estimated as, on applying Eq. (8),

$$\Psi_k^{(\text{est})}(N) = \frac{2\pi}{N} \sum_{l=0}^{N-1} e^{ik\vartheta_l} \frac{1}{n(\vartheta_l)} \sum_{r=1}^{n(\vartheta_l)} K_k[x_r(\vartheta_l)], \quad (57)$$

where  $x_r(\vartheta_l)$  is the result of the  $r$ th individual measurement at the phase  $\vartheta_l$ . Taking the average of all estimates  $\overline{\Psi_k^{(\text{est})}(N)}$ ,

$$\overline{\Psi_k^{(\text{est})}(N)} = \frac{2\pi}{N} \sum_{l=0}^{N-1} e^{ik\vartheta_l} \frac{1}{n(\vartheta_l)} \sum_{r=1}^{n(\vartheta_l)} \overline{K_k[x_r(\vartheta_l)]}, \quad (58)$$

yields, as expected,  $\Psi_k(N)$  from Eq. (49),

$$\overline{\Psi_k^{(\text{est})}(N)} = \Psi_k(N), \quad (59)$$

because of

$$\overline{K_k(x_r(\vartheta_l))} = \int_{-\infty}^{\infty} dx K_k(x) p(x, \vartheta_l). \quad (60)$$

The variances of the real and imaginary parts of  $\Psi_k^{(\text{est})}(N)$  can be obtained in a similar way. Taking into account that the individual measurements are independent of each other, we derive

$$\text{Var}\{\text{Re}[\Psi_k^{(\text{est})}(N)]\} = \frac{4\pi^2}{N^2} \sum_{l=0}^{N-1} \frac{\cos^2(k\vartheta_l)}{n(\vartheta_l)} \overline{\{\Delta K_k[x_r(\vartheta_l)]\}^2}, \quad (61)$$

and

$$\text{Var}\{\text{Im}[\Psi_k^{(\text{est})}(N)]\} = \frac{4\pi^2}{N^2} \sum_{l=0}^{N-1} \frac{\sin^2(k\vartheta_l)}{n(\vartheta_l)} \overline{\{\Delta K_k[x_r(\vartheta_l)]\}^2}, \quad (62)$$

where

$$\overline{\{\Delta K_k[x_r(\vartheta_l)]\}^2} = \int_{-\infty}^{\infty} dx K_k^2(x) p(x, \vartheta_l) - \left[ \int_{-\infty}^{\infty} dx K_k(x) p(x, \vartheta_l) \right]^2. \quad (63)$$

Equations (61) – (63) enable us to estimate the statistical error of the measured moments, substituting in Eqs. (61) and (62) for  $\overline{\{\Delta K_k[x_r(\vartheta_l)]\}^2}$  the corresponding estimates. From Eqs. (61) – (63) it is seen that the statistical error depends on the shape of the function  $K_k(x)$ . In order to reduce the statistical error, the ambiguity in the determination of  $K_k(x)$  can be advantageously used to choose it such that it varies as slowly as possible. This is one of the reasons

for omitting the polynomial in Eq. (28). Moreover, the statistical error can be reduced when the number of events,  $n(\vartheta_l)$ , is appropriately varied with the phase  $\vartheta_l$ . From Eqs. (61) and (62) it is suggested to increase  $n(\vartheta_l)$  for such phases for which  $\{\Delta K_k[x_r(\vartheta_l)]\}^2$ , Eq. (63), becomes relatively large. This is typically the case when  $p(x, \vartheta)$  is essentially nonzero in an  $x$  interval around  $x = 0$ , in which  $K_k(x)$  strongly varies with  $x$ . Note that this result is in qualitative agreement with that of the maximum-likelihood method for estimating phase shifts [21].

## 5 Computer simulations of measurements

### 5.1 Exponential phase moments

To illustrate the method, we have performed computer simulations of measurements of the quadrature component distribution  $p(x, \vartheta)$ , assuming the signal field to be prepared in various states, such as a squeezed vacuum  $|0\rangle_s = \hat{S}(\xi)|0\rangle = \exp\{-\frac{1}{2}[\xi(\hat{a}^\dagger)^2 - \xi^*\hat{a}^2]\}|0\rangle$  and a displaced Fock state  $|\alpha, n\rangle = \hat{D}(\alpha)|n\rangle = \exp(\alpha\hat{a}^\dagger - \alpha^*\hat{a})|n\rangle$ . We have restricted attention to perfect detection and assumed that the measurements are performed at  $N=120$  (equidistant) phases  $\vartheta_l$  within a  $2\pi$  interval and  $n(\vartheta_l) = 10^4$  events are recorded at each phase. Examples of the sampled exponential phase moments  $\Psi_k$  are shown in Figs. 4 and 5 for a squeezed vacuum and a displaced Fock state, respectively. The error bars indicate the standard deviations obtained according to Eqs. (61) and (62). Compared to the statistical error, the systematic error due to phase discretization is (for the chosen number  $N$  of phases  $\vartheta_l$ ) negligible small. From Figs. 4 and 5 we see that [for the chosen numbers  $n(\vartheta_l)$  of events] the exponential phase moments are obtained with sufficiently good accuracy, provided that  $k$  is small enough. We further see that the accuracy decreases with increasing  $k$ . (Note that for the chosen state parameters the imaginary parts must vanish for all  $k$ .) Clearly, the accuracy can be improved if the number of measurements is increased.

### 5.2 Phase distribution

The possibility of direct sampling of exponential phase moments  $\Psi_k$  offers novel possibilities of experimental verification of fundamental number-phase uncertainty relations, as has been shown recently [15]. It is worth noting that the measurements can be performed with high precision since only low-order moments play a role. Here we address the problem of the determination of the whole phase distribution  $P(\varphi)$ .

Since the exponential phase moments are nothing but the Fourier components of the phase distribution [Eq. (5)], the sampled moments can be used to



reconstruct the phase distribution according to

$$P(\varphi) = \frac{1}{2\pi} \sum_{k=-\infty}^{\infty} e^{-ik\varphi} \Psi_k. \quad (64)$$

Moreover, since any physical quantum state can be approximated to any desired degree of accuracy by truncating it at some photon number  $n_{\max}$  if  $n_{\max}$  is suitably large, from Eq. (20) it follows that (for chosen accuracy) the number of moments  $\Psi_k$  that effectively contribute to  $P(\varphi)$  in Eq. (64) is finite, i.e.,  $|k| = 1, 2, \dots, K$ , with  $K = n_{\max}$ . Hence,  $P(\varphi)$  can be obtained truncating the sum in Eq.(64) at  $|k| = K$  and substituting for the  $\Psi_k$  the measured moments  $\Psi_k^{(\text{est})}$ . The phase distributions that are reconstructed from the measured moments given in Figs. 4 and 5 for a squeezed vacuum and a displaced Fock state, respectively, are plotted in Fig. 6, on assuming that  $n_{\max}=20$ . The statistical error of  $\Psi_k^{(\text{est})}$  gives of course rise to an error of  $P(\varphi)$ . Since the error in  $P(\varphi)$  can be obtained easily from the law of error propagation [22] in a standard way, we renounce the calculation here.

Finally, it should be pointed out that there are other methods, such as least-squares inversion [23, 22] and maximum-entropy inversion [24], which can be used for reconstructing the phase distribution from the measured (i.e., inaccurate) exponential phase moments – methods that have been successfully applied in various fields of physics. Let us briefly comment on the application of the method of least-squares inversion. For this purpose we return to Eq. (5) and ask for  $P(\varphi)$  that best fits the experimental data at  $M$  chosen phases  $\varphi_m$  ( $m = 0, 1, \dots, M-1$ , with  $M \gg 2K$ ). An answer can be given applying the method of least-squares inversion [23, 22] to the set of  $2K$  linear equations for  $M$  unknown  $P(\varphi_m)$  ( $\varphi_m = 2\pi m/M$ ),

$$\text{Re } \Psi_k = \frac{2\pi}{M} \sum_{m=0}^{M-1} \cos(k\varphi_m) P(\varphi_m), \quad (65)$$

$$\text{Im } \Psi_k = \frac{2\pi}{M} \sum_{m=0}^{M-1} \sin(k\varphi_m) P(\varphi_m) \quad (66)$$

( $k = 1, 2, \dots, K$ ), i.e., minimizing the functional

$$\chi^2 = \sum_{k=1}^K \left\{ \left[ \sigma_k^{(\text{Re})} \right]^{-2} \left[ \text{Re } \Psi_k^{(\text{est})} - \frac{2\pi}{M} \sum_{m=0}^{M-1} P(\varphi_m) \cos(k\varphi_m) \right]^2 + \left[ \sigma_k^{(\text{Im})} \right]^{-2} \left[ \text{Im } \Psi_k^{(\text{est})} - \frac{2\pi}{M} \sum_{m=0}^{M-1} P(\varphi_m) \sin(k\varphi_m) \right]^2 \right\}, \quad (67)$$

where  $\sigma_k^{(\text{Re})}$  and  $\sigma_k^{(\text{Im})}$ , respectively, represent the errors involved in the determination of  $\text{Re } \Psi_k^{(\text{est})}$  and  $\text{Im } \Psi_k^{(\text{est})}$ . In particular, when  $\sigma_k^{(\text{Re})} \approx \sigma_k^{(\text{Im})} = \sigma$  then (for  $M \gg 2K$ ) the resulting  $P(\varphi_m)$  is in agreement with that obtained from Eq. (64),

with  $|k| \leq K$ . From comparison with the exact phase distribution it can be seen (Fig. 6) that outside the regions in which the phase distribution is essentially nonzero artificial oscillations and even negative values of the reconstructed distribution may be found, because of the statistical error of the measured moments (cf. Figs. 4 and 5). The problem can be partially overcome introducing regularization techniques in the solution of Eqs. (65) and (66) (for details, see [23]), as it can be seen from Fig. 6. The figure also reveals that the artifacts are suppressed at the expense of a smearing of the overall distribution.

## 6 Summary and conclusions

We have presented a method for direct sampling of the exponential moments of the canonical phase of a single-mode radiation field from the data recorded in balanced homodyning. The sampling method enables us to determine the moments in real time, together with the statistical error. It is worth noting that the method renders it possible to closely relate the basic-theoretical concept of canonical phase to the experiment. The sampling functions relating the quadrature-component distribution to the exponential phase moments are well behaved. With increasing quadrature-component they rapidly approach their classical counterparts given either by step functions (for odd moments) or logarithmic functions (for even moments). In this way the concept provides us with a unified approach to the experimental determination of the canonical phase in both quantum and classical optics.

In our approach to the construction of the kernel functions needed for direct sampling the exponential phase moments we have extended the proposal made in [18]. Hence the here used subtraction of the polynomial arbitrariness from the sampling functions can be considered as a significant improvement. In fact the omission of the ambiguity from the kernels provided us with functions that can be universally used for any physical state and that are much more insensitive to errors. This point should be also considered if a similar approach to the derivation of the kernel corresponding to any other generic field operator is adopted.

In order to study the accuracy of the method, we have discussed the influence of various experimental inaccuracies on the measured exponential phase moments. In particular, the finite number of local-oscillator phases results in an aliasing effect, whereas smearing of the quadrature-component causes a bias toward smaller absolute values of the moments. When the data smearing results from imperfect detection with efficiency larger 50%  $\eta$ , then modified sampling functions can be introduced for compensating the losses.

To illustrate the applicability of the method, we have performed computer simulations of measurements for two quantum states and presented the measured exponential phase moments including the statistical error. Finally, we have used the moments for a reconstruction of the whole phase distribution. The re-

sults obtained are in good agreement with the theoretical predictions.

## Acknowledgments

We are grateful to V. Peřinová for helpful and enlightening discussions. This work was supported by the Deutsche Forschungsgemeinschaft.

## Appendix A Derivation of Eqs. (28) – (31)

Combining Eqs. (19), (25), and (26) yields, provided that the moments and correlations  $\langle \hat{a}^{\dagger n} \hat{a}^m \rangle$  exist for all  $n$  and  $m$ ,

$$\Psi_k = \int_{2\pi} d\vartheta \int_{-\infty}^{\infty} dx \tilde{K}_k(x) e^{ik\vartheta} p(x, \vartheta), \quad (\text{A } 1)$$

where

$$\tilde{K}_k(x) = (2\pi)^{-1} \sum_{l=0}^{\infty} C_l^{(k)} H_{2l+k}(x), \quad (\text{A } 2)$$

with

$$C_l^{(k)} = \frac{(l+k)!}{2^{l+k/2}(2l+k)} \sum_{n=0}^l \binom{l}{n} \frac{(-1)^{l-n}}{\sqrt{(n+1) \dots (n+k)}}. \quad (\text{A } 3)$$

Using the relation

$$\frac{1}{\sqrt{(n+1) \dots (n+k)}} = \frac{1}{\pi^{k/2}} \int_{-\infty}^{+\infty} dt_1 e^{-t_1^2} \dots \int_{-\infty}^{+\infty} dt_k e^{-kt_k^2} e^{-nr_k^2}, \quad (\text{A } 4)$$

where

$$r_k^2 = \sum_{j=1}^k t_j^2, \quad (\text{A } 5)$$

we may rewrite Eq. (A 3) as

$$\begin{aligned} C_l^{(2m+1)} &= \frac{(2m+1+l)!}{(2\pi)^{m+\frac{1}{2}}(2m+1+2l)!} \int_{-\infty}^{+\infty} dt_1 e^{-t_1^2} \dots \\ &\quad \times \dots \int_{-\infty}^{+\infty} dt_{2m+1} e^{-(2m+1)t_{2m+1}^2} z_{2m+1}^l \end{aligned} \quad (\text{A } 6)$$

and

$$C_l^{(2m)} = \frac{(2m+l)!}{(2\pi)^m(2m+2l)!} \int_{-\infty}^{+\infty} dt_1 e^{-t_1^2} \dots \int_{-\infty}^{+\infty} dt_{2m} e^{-2mt_{2m}^2} z_{2m}^l \quad (\text{A } 7)$$

for  $k = 2m+1$  and  $k = 2m$ , respectively, where

$$z_k = \frac{1}{2}(e^{-r_k^2} - 1). \quad (\text{A } 8)$$

We now substitute in Eq. (A 2) for  $C_l^{(k)}$  the expressions (A 6) and (A 7) and change the summation index  $l$  as  $m+l=j$ . In order to separate from  $\tilde{K}_k(x)$  an irrelevant polynomial  $F_k(x)$ , we decompose  $\tilde{K}_k(x)$  into two parts,

$$\tilde{K}_k(x) = K_k(x) - F_k(x), \quad (\text{A } 9)$$

on rewriting the  $j$  sum such that in  $F_k(x)$  it runs from  $j=0$  and  $j=1$ , respectively, to  $j=m-1$  for odd and even  $k$ . In this way we find that

$$\begin{aligned} K_{2m+1}(x) &= \frac{(m+1)!}{(2\pi)^{m+3/2}} \int_{-\infty}^{+\infty} dt_1 e^{-t_1^2} \dots \\ &\times \dots \int_{-\infty}^{+\infty} dt_{2m+1} \frac{e^{-(2m+1)t_{2m+1}^2}}{z_{2m+1}^m} \sum_{j=0}^{\infty} \frac{\Gamma(m+2+j) z_{2m+1}^j}{(2j+1)! \Gamma(m+2)} H_{2j+1}(x) \end{aligned} \quad (\text{A } 10)$$

and

$$\begin{aligned} K_{2m}(x) &= \frac{m!}{(2\pi)^{m+1}} \int_{-\infty}^{+\infty} dt_1 e^{-t_1^2} \dots \\ &\times \dots \int_{-\infty}^{+\infty} dt_{2m} \frac{e^{-2mt_{2m}^2}}{z_{2m}^m} \left[ \sum_{j=0}^{\infty} \frac{\Gamma(m+1+j) z_{2m}^j}{(2j)! \Gamma(m+1)} H_{2j}(x) - 1 \right]. \end{aligned} \quad (\text{A } 11)$$

The polynomial  $F_k(x)$  can be written as

$$\begin{aligned} F_k(x) &= \frac{1}{(2\pi)^{1+k/2}} \\ &\times \sum_{n=1}^{\lfloor \frac{k-1}{2} \rfloor} \frac{(k-n)!}{(k-2n)!} H_{k-2n}(x) \int_{-\infty}^{+\infty} dt_1 e^{-t_1^2} \dots \int_{-\infty}^{+\infty} dt_k \frac{e^{-kt_k^2}}{z_k^n}, \end{aligned} \quad (\text{A } 12)$$

where the summation index  $j$  has been changed as  $m-j=n$ . Next we apply the sum rules [25]

$$\sum_{j=0}^{\infty} \frac{\Gamma(a+j) z^j}{(2j)! \Gamma(a)} H_{2j}(x) = \frac{1}{(1+z)^a} \Phi[a, 1/2, x^2 z / (1+z)], \quad (\text{A } 13)$$

$$\sum_{j=0}^{\infty} \frac{\Gamma(a+j) z^j}{(2j+1)! \Gamma(a)} H_{2j+1}(x) = \frac{2x}{(1+z)^a} \Phi[a, 3/2, x^2 z / (1+z)] \quad (\text{A } 14)$$

[ $|z| < 1$ ;  $\Phi(a, b, y)$ , confluent hypergeometric function] to the  $j$  sums in Eqs. (A 10) and (A 11) and obtain

$$\begin{aligned} K_{2m+1}(x) &= \frac{2x(m+1)!}{(2\pi)^{m+3/2}} \int_{-\infty}^{+\infty} dt_1 e^{-t_1^2} \dots \\ &\times \dots \int_{-\infty}^{+\infty} dt_{2m+1} e^{-(2m+1)t_{2m+1}^2} \frac{\Phi[m+2, 3/2, z_{2m+1}(1+z_{2m+1})^{-1}x^2]}{z_{2m+1}^m (1+z_{2m+1})^{m+2}} \end{aligned} \quad (\text{A } 15)$$

$$K_{2m}(x) = \frac{m!}{(2\pi)^{m+1}} \int_{-\infty}^{+\infty} dt_1 e^{-t_1^2} \dots \\ \times \dots \int_{-\infty}^{+\infty} dt_{2m} e^{-2mt_{2m}^2} \left\{ \frac{\Phi[m+1, 1/2, z_{2m}(1+z_{2m})^{-1}x^2]}{z_{2m}^m (1+z_{2m})^{m+1}} - \frac{1}{z_{2m}^m} \right\} \quad (\text{A } 16)$$

To write the multidimensional integrals in Eqs. (A 15) and (A 16) in a more compact form, we change the variables as, on using generalized spherical coordinates

$$t_i = r \cos \varphi_i \prod_{j=1}^{i-1} \sin \varphi_j \quad \text{if } i < k, \quad \text{and} \quad t_k = r \prod_{j=1}^{k-1} \sin \varphi_j, \quad (\text{A } 17)$$

and  $r = r_k$ , with  $0 \leq r < \infty$ ,  $0 \leq \varphi_j \leq \pi$  if  $j < k-1$ , and  $0 \leq \varphi_{k-1} \leq 2\pi$ . Introducing the function

$$\Omega^{(k)}(r^2) = \int_0^\pi d\varphi_1 e^{-t_1^2} \sin^{k-2} \varphi_1 \dots \int_0^\pi d\varphi_j e^{-j t_j^2} \sin^{k-j-1} \varphi_j \dots \\ \times \dots \int_0^{2\pi} d\varphi_{k-1} e^{-(k-1)t_{k-1}^2} e^{-kt_k^2} \quad (\text{A } 18)$$

and recalling Eq. (A 8) [together with Eq. (A 5)], we find that Eqs. (A 15) and (A 16) can be rewritten as given in Eqs. (29) and (30) in Sec. 3. Finally, we expand in Eq. (A 12)  $z_k^{-n}$  as

$$\frac{1}{z_k^n} = \frac{(-2)^n}{(1 - e^{-r_k^2})^n} = (-2)^n \sum_{l=0}^{\infty} \frac{(n+l-1)!}{l!(n-1)!} e^{-lr_k^2} \quad (\text{A } 19)$$

and perform the Gaussian integrals to obtain  $F_k(x)$  in the form of Eq. (31) in Sec. 3.

## Appendix B Derivation of Eqs. (32) and (33)

In order to write the function  $\Omega^{(k)}(z)$  in the form of Eq. (32) together with Eq. (33), we first rewrite Eq. (A 18) as

$$\Omega^{(k)}(r^2) = \int_0^\pi d\varphi_1 \sin^{k-2} \varphi_1 \dots \int_0^\pi d\varphi_i \sin^{k-i-1} \varphi_i \dots \int_0^{2\pi} d\varphi_{k-1} e^{-X_k}, \quad (\text{B } 1)$$

where

$$X_k = t_1^2 + 2t_2^2 + \dots + kt_k^2, \quad (\text{B } 2)$$

$t_k$  being given in Eq. (A 17). We then expand the exponential  $e^{-X_k}$  in a power series, which implies the power-series expansion of  $\Omega^{(k)}(r^2)$ ,

$$\Omega^{(k)}(r^2) = \sum_{m=0}^{\infty} A_m^{(k)} r^{2m}. \quad (\text{B } 3)$$

Here, the expansion coefficients  $A_m^{(k)}$  are given by

$$A_m^{(k)} = \frac{(-1)^m}{m!} \int_0^\pi d\varphi_1 \sin^{k-2} \varphi_1 \cdots \int_0^\pi d\varphi_i \sin^{k-i-1} \varphi_i \cdots \int_0^{2\pi} d\varphi_{k-1} Y_k^m, \quad (\text{B } 4)$$

where  $Y_k = X_k/r^2$  is an  $r$ -independent angular function,  $Y_k = Y_k(\varphi_j)$ . Particular integrals of the type given in Eq. (B 4) are calculated in [25]. They can be used to prove, by induction, that for arbitrary  $k$  and  $m$  the coefficients  $A_m^{(k)}$  can be written in the form given in Eq. (33).

## Appendix C Asymptotics of $K_k(x)$

In order to find the asymptotic behaviour of  $K_k(x)$  for large  $x$ , we change the variables in the integrals in Eqs. (29) and (30) according to  $\tanh(r^2/2) = \gamma$  and obtain

$$K_{2m+1}(x) = x \int_0^1 d\gamma D^{(2m+1)}(\gamma) \Phi(m+2, \frac{3}{2}, -\gamma x^2) \quad (\text{C } 1)$$

and

$$K_{2m}(x) = \int_0^1 d\gamma D^{(2m)}(\gamma) \left[ \Phi(m+1, \frac{1}{2}, -\gamma x^2) - (1+\gamma)^{-(m+1)} \right], \quad (\text{C } 2)$$

where

$$\begin{aligned} D^{(2m+1)}(\gamma) &= \frac{2(-1)^m (m+1)!}{(2\pi)^{m+3/2}} \left[ \ln \left( \frac{1+\gamma}{1-\gamma} \right) \right]^{m-1/2} \\ &\times \Omega^{(2m+1)} \left[ \ln \left( \frac{1+\gamma}{1-\gamma} \right) \right] \frac{(1+\gamma)^{2m+1}}{\gamma^m (1-\gamma)}, \end{aligned} \quad (\text{C } 3)$$

$$\begin{aligned} D^{(2m)}(\gamma) &= \frac{(-1)^m m!}{(2\pi)^{m+1}} \left[ \ln \left( \frac{1+\gamma}{1-\gamma} \right) \right]^{m-1} \\ &\times \Omega^{(2m)} \left[ \ln \left( \frac{1+\gamma}{1-\gamma} \right) \right] \frac{(1+\gamma)^{2m}}{\gamma^m (1-\gamma)}. \end{aligned} \quad (\text{C } 4)$$

Let us first draw attention to  $K_{2m+1}(x)$  in Eq. (C 1). For  $\gamma > 0$  the function  $D^{(2m+1)}(\gamma)$  is finite, and from the asymptotic behaviour of  $\Omega^{(k)}(r^2)$  for large  $r$  it follows that  $D^{(2m+1)}(1) = 0$ . From the asymptotic behaviour of the confluent hypergeometric function,

$$\Phi(a, c, -t) \approx \frac{\Gamma(c)}{\Gamma(c-a)} \frac{1}{t^a}, \quad t \rightarrow \infty, \quad (\text{C } 5)$$

it follows that  $\Phi(m+2, \frac{3}{2}, -\gamma x^2) \rightarrow 0$  if  $|x| \rightarrow \infty$  except for  $\gamma = 0$ . Hence, for  $|x| \gg 1$  we can approximate the integral in Eq. (C 1), replacing  $D^{(2m+1)}(\gamma)$  with its expansion for  $\gamma \ll 1$ . Taking into account that

$$\ln\left(\frac{1+\gamma}{1-\gamma}\right) = 2\gamma \left[1 + \mathcal{O}(\gamma^2)\right] \quad (\text{C } 6)$$

and recalling the expansion of  $\Omega^{(k)}(z)$ , Eqs. (32) and (33), we find that

$$\Omega^{(k)}\left[\ln\left(\frac{1+\gamma}{1-\gamma}\right)\right] = \frac{2\pi^{k/2}}{\Gamma(k/2)} \left[1 - (k+1)\gamma + \mathcal{O}(\gamma^2)\right]. \quad (\text{C } 7)$$

Thus, for  $\gamma \ll 1$  the function  $D^{(2m+1)}(\gamma)$ , Eq. (C 3), can be given by

$$D^{(2m+1)}(\gamma) = \frac{(-1)^m(m+1)!}{\pi\Gamma(m+1/2)} \gamma^{-1/2} \left[1 + \mathcal{O}(\gamma^2)\right], \quad \gamma \ll 1, \quad (\text{C } 8)$$

so that Eq. (C 1) for  $x \gg 1$  can be written as, on changing the variables as  $\gamma^{1/2}x = t$ ,

$$\begin{aligned} K_{2m+1}(x) &= \frac{2(-1)^m(m+1)!}{\pi\Gamma(m+1/2)} \int_0^x dt \left[1 + \mathcal{O}(t^4/x^4)\right] \Phi(m+2, \frac{3}{2}, -t^2) \\ &= \frac{2(-1)^m(m+1)!}{\pi\Gamma(m+1/2)} \left\{ I^{(1)}(0) - I^{(1)}(x) + \mathcal{O}(x^{-4}) \left[ I^{(2)}(0) - I^{(2)}(x) \right] \right\}, \end{aligned} \quad (\text{C } 9)$$

where the abbreviating notations

$$I^{(1)}(x) = \int_x^\infty dt \Phi(m+2, \frac{3}{2}, -t^2) \quad (\text{C } 10)$$

and

$$I^{(2)}(x) = \int_x^\infty dt t^4 \Phi(m+2, \frac{3}{2}, -t^2) \quad (\text{C } 11)$$

have been introduced. The integral  $I^{(1)}(0)$  can be calculated to be [26]

$$I^{(1)}(0) = \int_0^\infty dt \Phi(m+2, \frac{3}{2}, -t^2) = \frac{\pi(2m+1)}{8(m+1)!} \Gamma[(2m+1)/2] \quad (\text{C } 12)$$

and it can be shown that  $I^{(2)}(0)=0$ . Further, from Eq. (C 5) it follows that  $I^{(1)}(x) = \mathcal{O}(x^{-2m+1})$  and  $I^{(2)}(x) = \mathcal{O}(x^{-2m+1})$ . For  $x < 0$  ( $|x| \gg 1$ ) the calculations are quite analogous, so that

$$K_{2m+1}(x) = \frac{1}{4}(-1)^m(2m+1) \text{sign}(x) \left[1 + \mathcal{O}(x^{-2m-3})\right], \quad |x| \gg 1. \quad (\text{C } 13)$$

To find the asymptotic behaviour of  $K_{2m}(x)$ , we subdivide the interval of integration in Eq. (C 2) as

$$K_{2m}(x) = I(0, M/x^2) + I(M/x^2, \gamma_0) + I(\gamma_0, 1), \quad (\text{C } 14)$$

where

$$I(a, b) = \int_a^b d\gamma D^{(2m)}(\gamma) \left[ \Phi(m+1, \tfrac{1}{2}, -\gamma x^2) - (1+\gamma)^{-m-1} \right], \quad (\text{C } 15)$$

and  $\gamma_0 \ll 1$  and  $M \gg 1$  such that  $M/x^2 < \gamma_0$ . This reflects the qualitatively different behaviour of the integrand in these intervals. In the integrals  $I(0, M/x^2)$  and  $I(M/x^2, \gamma_0)$  the variable  $\gamma$  is small, so that  $D^{(2m)}(\gamma)$  can be expanded as, on using Eqs. (C 6) and (C 7),

$$D^{(2m)}(\gamma) = (2\pi)^{-1}(-1)^m m \gamma^{-1} \left[ 1 + \mathcal{O}(\gamma^2) \right], \quad \gamma \ll 1. \quad (\text{C } 16)$$

We also expand  $(1+\gamma)^{-m-1}$  and can rewrite  $I(0, M/x^2)$  as (after changing the variables)

$$I(0, M/x^2) = C_1(M) + \mathcal{O}(M/x^2), \quad (\text{C } 17)$$

where

$$C_1(M) = (2\pi)^{-1}(-1)^m m \int_0^M \frac{dt}{t} \left[ \Phi(m+1, \tfrac{1}{2}, -t) - 1 \right]. \quad (\text{C } 18)$$

$I(M/x^2, \gamma_0)$  and  $I(\gamma_0, 1)$  can be calculated integrating the two terms in Eq. (C 14) separately. Recalling Eq. (C 5) and changing the variables, we find that  $I(M/x^2, \gamma_0) = I^{(a)} + I^{(b)}$ , with

$$\begin{aligned} I^{(a)} &= (2\pi)^{-1}(-1)^m m \int_M^{\gamma_0 x^2} \frac{dt}{t} \left[ 1 + \mathcal{O}(t^2/x^4) \right] \Phi(m+1, \tfrac{1}{2}, -t) \\ &= \mathcal{O}[(\gamma_0 x^2)^{-m-1}] + C_2(M), \end{aligned} \quad (\text{C } 19)$$

where  $C_2(M) = \mathcal{O}(M^{-m-1})$ , and [after expanding  $(1+\gamma)^{-m-1}$ ]

$$\begin{aligned} I^{(b)} &= (2\pi)^{-1}(-1)^m m \int_{M/x^2}^{\gamma_0} \frac{d\gamma}{\gamma} \left[ 1 + \mathcal{O}(\gamma^2) \right] [1 + \mathcal{O}(\gamma)] \\ &= \pi^{-1}(-1)^{m+1} m \ln |x| + C_3(M) + C_4(\gamma_0) + \mathcal{O}(M/x^2), \end{aligned} \quad (\text{C } 20)$$

where

$$C_3(M) = \pi^{-1}(-1)^{m+1} m \ln M, \quad (\text{C } 21)$$

$$C_4(\gamma_0) = (2\pi)^{-1}(-1)^{m+1} m [\ln \gamma_0 + \mathcal{O}(\gamma_0)]. \quad (\text{C } 22)$$

Finally,  $I(\gamma_0, 1)$  can be written as, on using Eq. (C 5),

$$\begin{aligned} I(\gamma_0, 1) &= \int_{\gamma_0}^1 d\gamma D^{(2m)}(\gamma) \left\{ \mathcal{O}[(\gamma x^2)^{-m-1}] - (1+\gamma)^{-m-1} \right\} \\ &= C_5(\gamma_0) + \mathcal{O}(\gamma_0^{-m} x^{-2m-2}), \end{aligned} \quad (\text{C } 23)$$



where

$$C_5(\gamma_0) = - \int_{\gamma_0}^1 d\gamma D^{(2m)}(\gamma) (1 + \gamma)^{-m-1}. \quad (\text{C } 24)$$

Substituting in Eq. (C 14) for  $I(0, M/x^2)$ ,  $I(M/x^2, \gamma_0)$  and  $I(\gamma_0, 1)$  the expressions derived above, it can be shown that the logarithmic divergences of  $C_4(\gamma_0)$  and  $C_5(\gamma_0)$  cancel for  $\gamma_0 \rightarrow 0$  and those of  $C_3(M)$  and  $C_1(M)$  cancel for  $M \rightarrow \infty$ , and hence

$$K_{2m}(x) = \pi^{-1}(-1)^{m+1}m \ln |x| + \mathcal{O}(M/x^2) + \mathcal{O}[(\gamma_0 x^2)^{-m-1}] + C(\gamma_0, M), \quad |x| \gg 1. \quad (\text{C } 25)$$

Here, the constant  $C(\gamma_0, M)$  is given by the sum of the constants  $C_1 - C_5$ . Note that for  $\gamma_0 \rightarrow 0$  and  $M \rightarrow \infty$  the constant  $C(\gamma_0, M)$  becomes independent on  $\gamma_0$  and  $M$  [for a determination of this irrelevant constant the value of the integral (C 24) must be known].

\* Permanent address: Palacký University, Faculty of Natural Sciences, Svobody 26, 77146 Olomouc, Czech Republic

## References

- [1] P.M.A. Dirac, Proc. Roy. Soc. A **114** (1927) 234.
- [2] A. Lukš and V. Peřinová, Quantum Opt. **6** (1994) 125; R. Lynch, Phys. Rep. **256** (1995) 367; A. Royer, Phys. Rev. A **53** (1996) 70; D.T. Pegg and S.M. Barnett, J. Mod. Opt. **44** (1997) 225.
- [3] U. Leonhardt, J.A. Vaccaro, B. Böhmer and H. Paul, Phys. Rev. A **51** (1995) 84.
- [4] F. London, Z. Phys. **40** (1927) 193.
- [5] N.G. Walker and J.E. Carroll, Opt. Quant. Electron. **18** (1986) 355; N.G. Walker, J. Mod. Opt. **34** (1987) 15; M. Freyberger, K. Vogel and W. Schleich, Phys. Lett. **176A** (1993), 41; U. Leonhardt and H. Paul, Phys. Rev. A **48** (1993) 4598.
- [6] J.W. Noh, A. Fougères and L. Mandel, Phys. Rev. Lett. **67** (1991) 1426; Phys. Rev. A **45** (1992) 424; Phys. Rev. A **46** (1992) 2840.
- [7] For the relation between the quadrature-component distribution and the quantum state, see K. Vogel and H. Risken, Phys. Rev. A **40** (1989) 2847.

- [8] D.T. Smithey, M. Beck, A. Faridani and M.G. Raymer, Phys. Rev. Lett. **70** (1993) 1244; D.T. Smithey, M. Beck, J. Cooper, M.G. Raymer and A. Faridani, Physica Scripta T**48** (1993) 35; G. Breitenbach, T. Müller, S.F. Pereira, J.-Ph. Poizat, S. Schiller and J. Mlynek, JOSA B **12** (1995) 2304.
- [9] G.M. D'Ariano, C. Macchiavello and M.G.A. Paris, Phys. Rev. A **50** (1994) 4298; U. Leonhardt, H. Paul and G.M. D'Ariano, Phys. Rev. A **52** (1995) 4899; M. Munroe, D. Boggavarapu, M.E. Anderson and M.G. Raymer, Phys. Rev. A **52** (1995) R924; S. Schiller, G. Breitenbach, S.F. Pereira, T. Müller and J. Mlynek, Phys. Rev. Lett. **77** (1996) 2933; U. Leonhardt, M. Munroe, T. Kiss, Th. Richter and M.G. Raymer, Opt. Commun. **127** (1996) 144; Th. Richter, Phys. Lett. **211A** (1996) 327;
- [10] Th. Richter, Phys. Rev. A **53** (1996) 1197.
- [11] D.T. Smithey, M. Beck, J. Cooper and M.G. Raymer, Phys. Rev. A **48** (1993) 3159.
- [12] G. Breitenbach and S. Schiller, J. Mod. Optics, to be published; G. Breitenbach, S. Schiller and J. Mlynek, Nature **387**, (1997) 471.
- [13] M. Dakna, L. Knöll and D.-G. Welsch, *Proceedings of the 4th Central-European Workshop on Quantum Optics* (Budmerice 1996), ed. V. Bužek [Act. Phys. Slov. **46** (1996) 349]; Quantum Semiclass. Opt. **9** (1997) 331; Phys. Rev. A **55** (1997) 2360.
- [14] S.M. Barnett and D.T. Pegg, Phys. Rev. Lett **76** (1996) 4148.
- [15] T. Opatrný, M. Dakna and D.-G. Welsch, submitted to Phys. Rev. A.
- [16] L. Susskind and J. Glogower, Physics **1** (1964) 49; P. Carruthers and M.M. Nieto, Phys. Rev. Lett. **14** (1965) 387, Rev. Mod. Phys. **40** (1968) 411.
- [17] W. Vogel and D.-G. Welsch, *Lectures on Quantum Optics* (Akademie Verlag, Berlin, 1994).
- [18] G.M. D'Ariano, in: *Quantum Communication, Computing and Measurement*, eds. O. Hirota, A.S. Holevo and C.M. Caves (Plenum, 1997).
- [19] U. Leonhardt and M. Munroe, Phys. Rev. A **54** (1996) 3682.
- [20] T. Opatrný, D.-G. Welsch, S. Wallentowitz and W. Vogel, J. Mod. Optics, to be published.
- [21] Z. Hradil, R. Myška, T. Opatrný and J. Bajer, Phys. Rev. A **53** (1996) 3738.
- [22] Ph.R. Bevington *Data Reduction and Error analysis for the Physical Sciences* (McGraw-Hill, New York, 1969).

- [23] W.H. Press, S.A. Teukolsky, W.T. Vetterling, B.P. Flannery, *Numerical recipes* (Cambridge university press, 1992).
- [24] E.T. Jaynes, Phys. Rev. **106**, (1957) 620.
- [25] A.P. Prudnikov, Yu.A. Brychkov and O.J. Marichev, *Integral and Series*, Vol 1 and 2 (Gordon and Breach, New York, 1986).
- [26] A. Erdelyi, *Higher Transcendental Functions*, Batman Manuscript Project, Vol 1 (McGraw-Hill, New York, 1953).

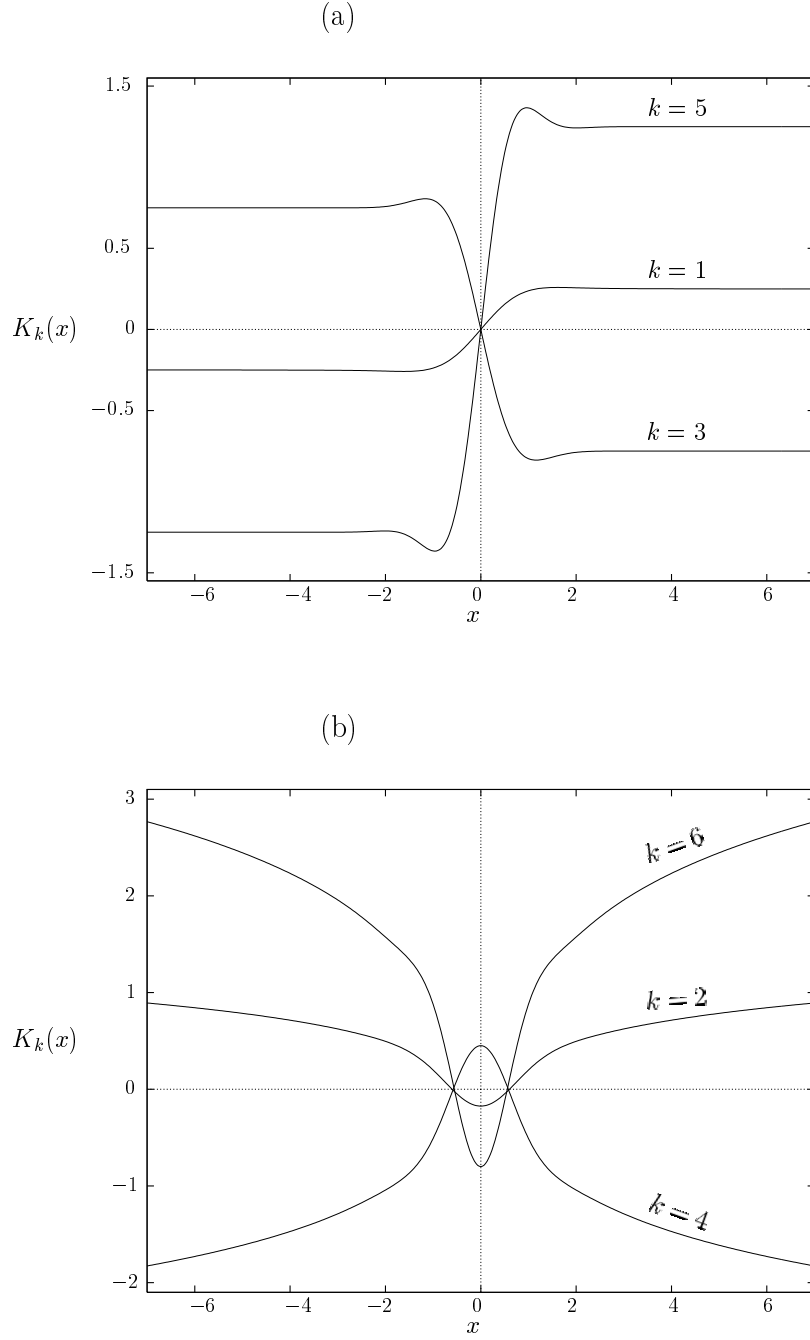


Figure 1: The  $x$ -dependent part  $K_k(x)$  of the sampling function  $K_k(x, \vartheta) = e^{ik\vartheta} K_k(x)$  for the determination of the exponential phase moments  $\Psi_k$  from the quadrature-component distribution  $p(x, \vartheta)$  is shown for various odd (a) and even (b)  $k$ .

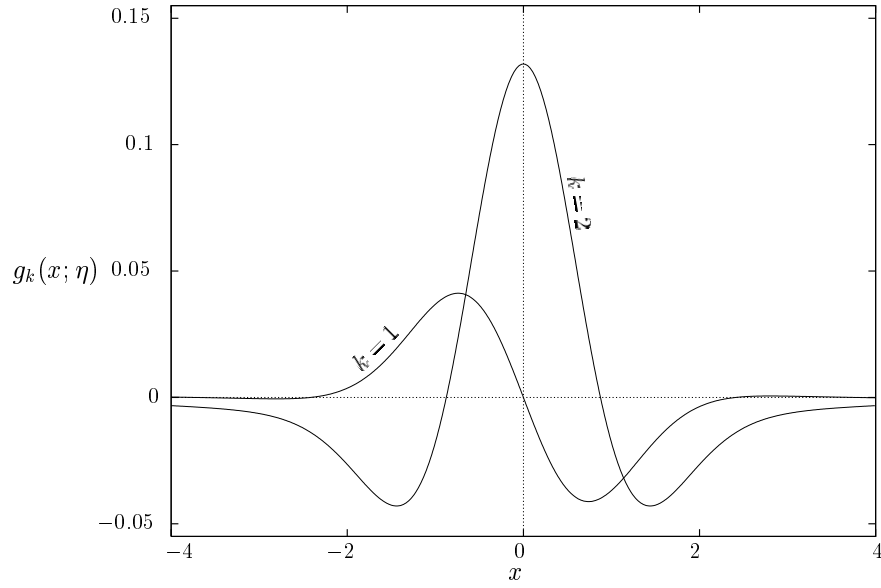


Figure 2: The function  $g_k(x; \eta)$  for the determination of the systematic error  $\Delta^{(s)}\Psi_k$ , Eq. (40), which is associated with Gaussian data smearing, is shown for  $k=1, 2$  and  $\eta=0.6$ .

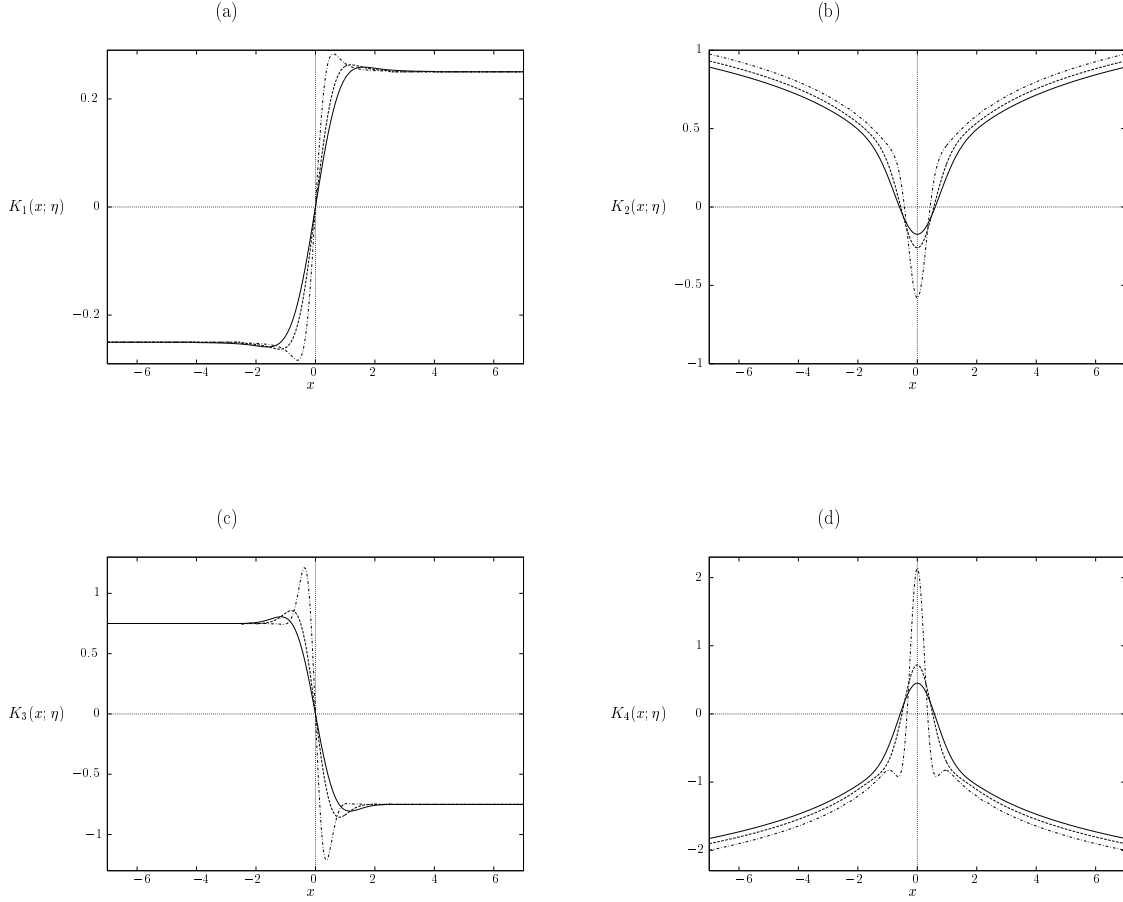


Figure 3: The  $x$ -dependent part  $K_k(x; \eta)$  of the sampling function  $K_k(x, \vartheta; \eta) = e^{ik\vartheta} K_k(x; \eta)$  for the determination of the exponential phase moments  $\Psi_k$  from the smeared quadrature-component distribution  $p(x, \vartheta; \eta)$  is shown for various  $k$  and  $\eta$  [ $\eta = 1$  (full lines),  $\eta = 0.8$  (dashed lines),  $\eta = 0.6$  (dashed-dotted lines)].

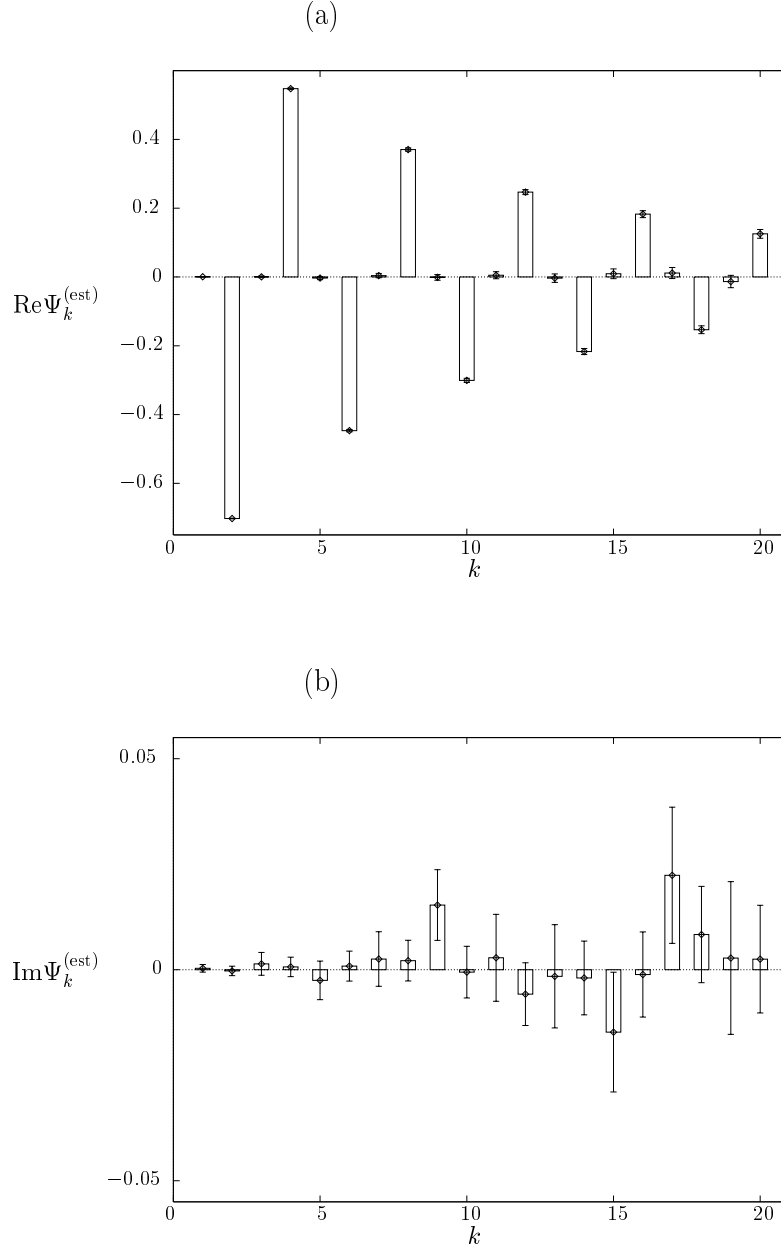


Figure 4: Examples of measured exponential phase moments  $\Psi_k^{(\text{est})}$  are shown for a mode prepared in a squeezed vacuum  $|0\rangle_s = \hat{S}(\xi)|0\rangle$ , with  $\xi = -1.31$ , i.e.,  $\langle \hat{n} \rangle = 3$  [(a) real part of  $\Psi_k^{(\text{est})}$ ; (b) imaginary part of  $\Psi_k^{(\text{est})}$ ]. The error bars indicate the estimated statistical error. In the computer simulation it is assumed that the quadrature component distribution  $p(x, \vartheta)$  is detected at 120 phases  $\vartheta$  equidistantly distributed in a  $2\pi$  interval and that at each phase  $10^4$  events are recorded.

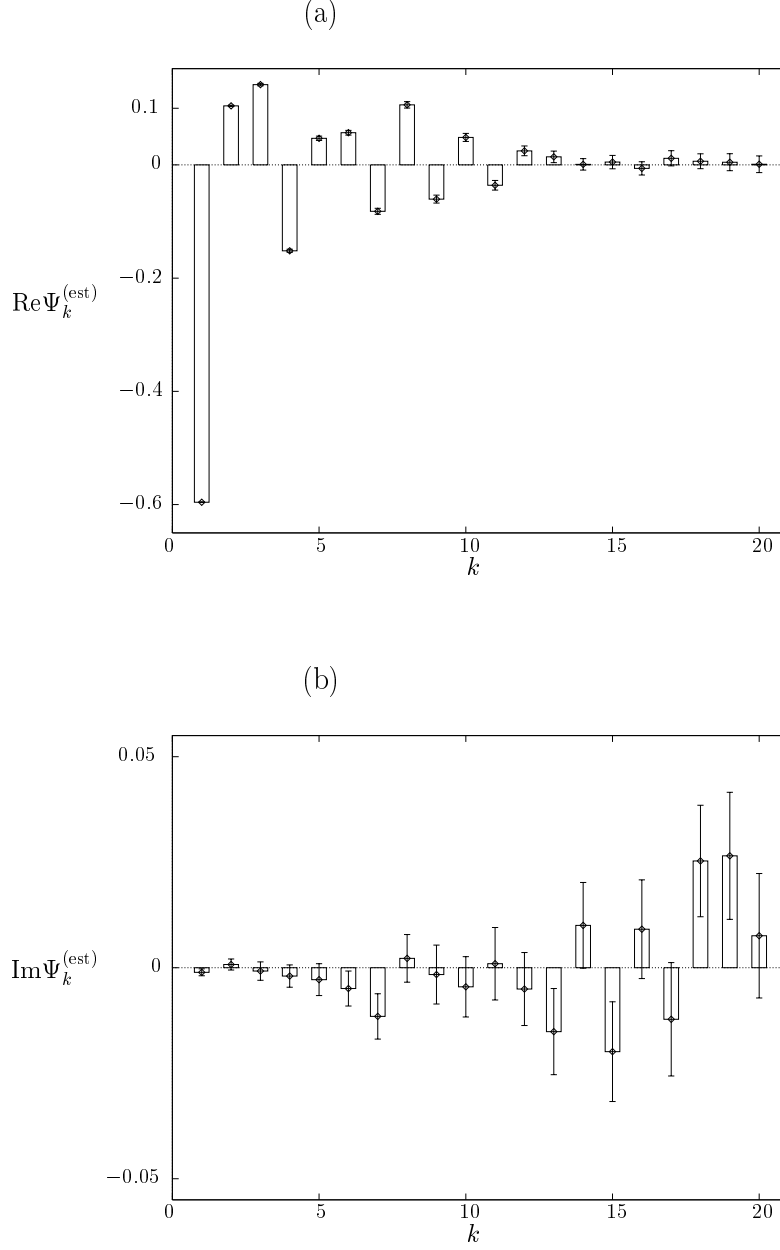


Figure 5: Examples of measured exponential phase moments  $\Psi_k^{(\text{est})}$  are shown for a mode prepared in a displaced Fock state  $|\alpha, n\rangle = \hat{D}(\alpha)|n\rangle$ , with  $\alpha = -1.5$  and  $n=2$ , i.e.,  $\langle \hat{n} \rangle = 4.25$  [(a) real part of  $\Psi_k^{(\text{est})}$ ; (b) imaginary part of  $\Psi_k^{(\text{est})}$ ]. The error bars indicate the estimated statistical error. In the computer simulation it is assumed that the quadrature component distribution  $p(x, \vartheta)$  is detected at 120 phases  $\vartheta$  equidistantly distributed in a  $2\pi$  interval and that at each phase  $10^4$  events are recorded.



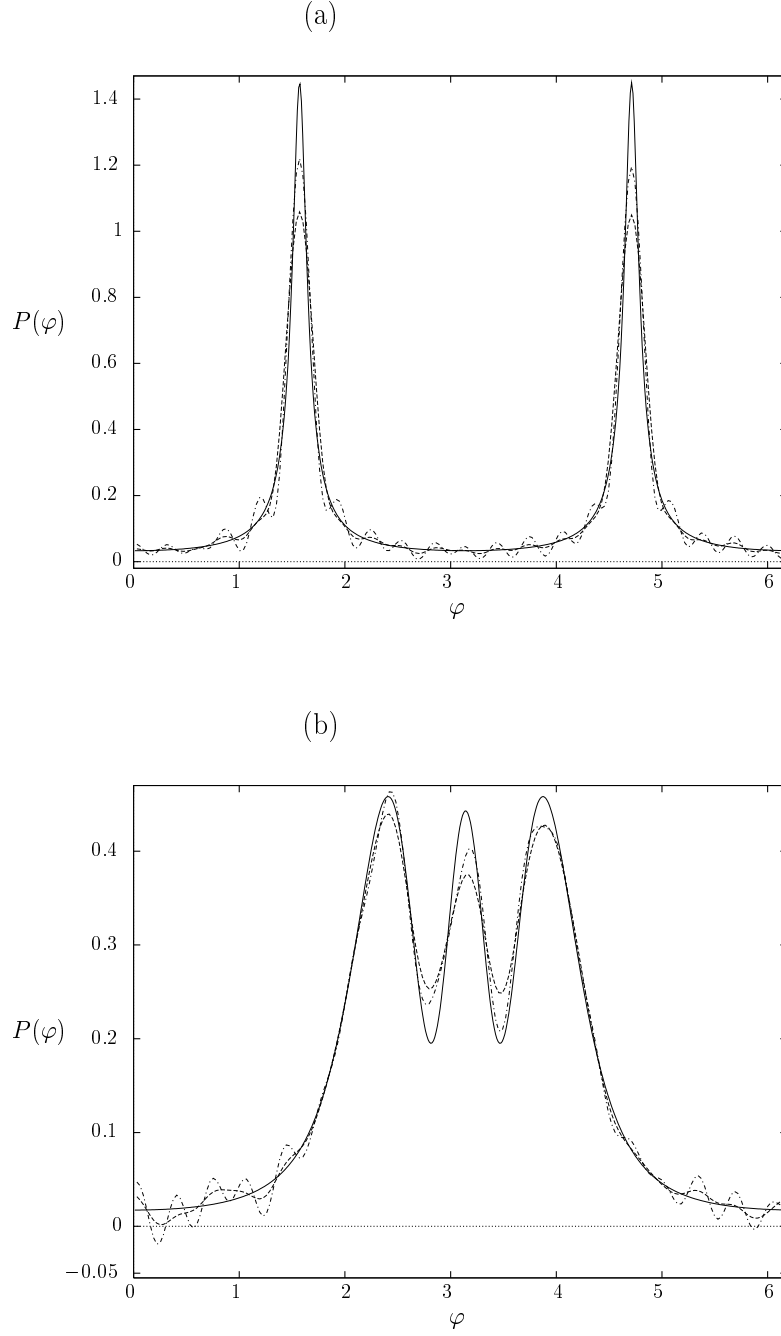


Figure 6: The canonical phase distribution  $P(\varphi)$  reconstructed from  $K = 20$  measured exponential phase moments  $\Psi_k^{(\text{est})}$  given in Figs. 4 and 5 is shown for the squeezed vacuum (a) and the displaced Fock state (b) therein. The results of direct application of Eq. (64) (dashed-dotted lines) and application of regularized least-squares inversion (dashed lines) are compared with the exact distributions (solid lines).